Journal of Controlled Release 358 (2023) 128–141

Contents lists available at ScienceDirect

Journal of Controlled Release

journal homepage: www.elsevier.com/locate/jconrel

Neutralisation of SARS-CoV-2 by monoclonal antibody through dual targeting powder formulation

Han Cong Seow [a,c,1], Jian-Piao Cai [b,1], Harry Weijie Pan [a], Cuiting Luo [b], Kun Wen [d], Jianwen Situ [b], Kun Wang [b], Hehe Cao [b], Susan W.S. Leung [a], Shuofeng Yuan [b,e,**], Jenny K. W. Lam [a,c,f,*]

[a] Department of Pharmacology and Pharmacy, LKS Faculty of Medicine, The University of Hong Kong, 21 Sassoon Road, Pokfulam, Hong Kong Special Administrative Region
[b] Department of Microbiology, LKS Faculty of Medicine, The University of Hong Kong, 21 Sassoon Road, Pokfulam, Hong Kong Special Administrative Region
[c] Department of Pharmaceutics, UCL School of Pharmacy, University College London, 29-39 Brunswick Square, WC1N 1AX, UK
[d] Microbiome Medicine Center, Division of Laboratory Medicine, Zhujiang Hospital, Southern Medical University, Guangzhou 510282, People's Republic of China
[e] Centre for Virology, Vaccinology and Therapeutics, Hong Kong Science and Technology Park, New Territories, Hong Kong Special Administrative Region
[f] Advanced Biomedical Instrumentation Centre, Hong Kong Science Park, Shatin, New Territories, Hong Kong Special Administrative Region

ARTICLE INFO

Keywords:
COVID-19
Intranasal delivery
Neutralising antibody, pulmonary delivery
Spray drying
Respiratory viral infections

ABSTRACT

Neutralising monoclonal antibody (mAb) is an important weapon in our arsenal for combating respiratory viral infections. However, the effectiveness of neutralising mAb has been impeded by the rapid emergence of mutant variants. Early administration of broad-spectrum mAb with improved delivery efficiency can potentially enhance efficacy and patient outcomes. WKS13 is a humanised mAb which was previously demonstrated to exhibit broad-spectrum activity against SARS-CoV-2 variants. In this study, a dual targeting formulation strategy was designed to deliver WKS13 to both the nasal cavity and lower airways, the two critical sites of infection caused by SARS-CoV-2. Dry powders of WKS13 were first prepared by spray drying, with cyclodextrin used as stabiliser excipient. Two-fluid nozzle (TFN) was used to produce particles below 5 μm for lung deposition (C-TFN formulation) and ultrasonic nozzle (USN) was used to produce particles above 10 μm for nasal deposition (C-USN formulation). Gel electrophoresis and size exclusion chromatography studies showed that the structural integrity of mAb was successfully preserved with no sign of aggregation after spray drying. To achieve dual targeting property, C-TFN and C-USN were mixed at various ratios. The aerosolisation property of the mixed formulations dispersed from a nasal powder device was examined using a Next Generation Impactor (NGI) coupled with a glass expansion chamber. When the ratio of C-TFN in the mixed formulation increased, the fraction of particles deposited in the lung increased proportionally while the fraction of particles deposited in the nasal cavity decreased correspondingly. A customisable aerosol deposition profile could therefore be achieved by manipulating the mixing ratio between C-TFN and C-USN. Dual administration of C-TFN and C-USN powders to the lung and nasal cavity of hamsters, respectively, was effective in offering prophylactic protection against SARS-CoV-2 Delta variant. Viral loads in both the lung tissues and nasal wash were significantly reduced, and the efficacy was comparable to systemic administration of unformulated WKS13. Overall, dual targeting powder formulation of neutralising mAb is a promising approach for prophylaxis of respiratory viral infections. The ease and non-invasive administration of dual targeting nasal powder may facilitate the widespread distribution of neutralising mAb during the early stage of unpredictable outbreaks.

* Correspondence to: Jenny K.W. Lam, Department of Pharmaceutics, UCL School of Pharmacy, University College London, 29-39 Brunswick Square, WC1N 1AX, United Kingdom.
** Correspondence to: Shuofeng Yuan, Department of Microbiology, LKS Faculty of Medicine, The University of Hong Kong, 21 Sassoon Road, Pokfulam, Hong Kong Special Administrative Region.
E-mail addresses: yuansf@hku.hk (S. Yuan), jenny.lam@ucl.ac.uk (J.K.W. Lam).
[1] These authors contributed equally to this manuscript.

https://doi.org/10.1016/j.jconrel.2023.04.029
Received 16 December 2022; Received in revised form 1 April 2023; Accepted 17 April 2023
Available online 30 April 2023

1. Introduction

The Coronavirus Disease 2019 (COVID-19) pandemic has clearly revealed the widespread and enduring impact of respiratory viral infections. Highly contagious viruses such as severe acute respiratory syndrome coronavirus 2 (SARS-CoV-2) are easily spread by patients with mild symptoms inadvertently, causing potentially fatal outcomes in patients with weak immune systems or comorbidities [1]. Despite rapid vaccine development and global health measures, the continual emergence of new mutant variants hinders the control of viral spread, rendering current treatment options ineffective [2,3]. Variants with enhanced resistance and transmissibility highlight the importance of implementing new approaches for prevention and treatment of COVID-19.

Current treatment of COVID-19 includes the use of anti-inflammatory drugs, antivirals, and monoclonal antibodies (mAbs) [4]. Neutralising mAbs, which are almost exclusively designed to target the receptor binding domain (RBD) of SARS-CoV-2 spike protein and block viral entry into host cells, had significant success in improving clinical outcomes. Several mAb therapeutics have been approved for prophylaxis or treatment of COVID-19 [5,6]. Since SARS-CoV-2 primarily infect the respiratory epithelium where they replicate and propagate [7], high concentration of neutralising mAbs in the airway epithelium is crucial for effective antiviral effect. Currently approved mAbs are delivered through parenteral administration which is suboptimal due to the poor transportation of these large protein molecules across the respiratory epithelium to the airways. Moreover, this administration route is invasive and logistically challenging for use in outpatients, especially when early administration (within the first few days of clinical infection) is key for effective treatment by neutralising mAbs. To improve the delivery of mAbs, several studies have demonstrated the therapeutic efficacy of mAbs through inhalation or intranasal administration, which markedly increased mAb concentration in the respiratory tract for local neutralisation action [8–10]. Aerosol delivery may also reduce the dose required and minimise the risks of systemic immunotoxicity [11].

WKS13 is a broad-spectrum humanised mAb that was recently discovered to exhibit potent neutralisation activity against different SARS-CoV-2 variants in hamsters through intraperitoneal administration [manuscript under revision]. The aim of this study was to develop an optimal formulation of WKS13 for potential clinical application by employing the dual targeting formulation strategy [12], in which a dry powder aerosol can be deposited in both the upper and lower respiratory tract simultaneously for antiviral activity through intranasal administration. A dual targeting formulation which contained particles with bimodal size distribution was prepared by blending spray dried powder of WKS13 of two different particle sizes, with the large particles (> 10 μm) for nasal deposition whilst the small particles (< 5 μm) for lung deposition. Cyclodextrin was used as the major excipient as it has been demonstrated to be an effective stabiliser to preserve protein activity during spray drying [13,14], with leucine added to the formulation in attempt to improve powder dispersibility [15]. The physicochemical properties and aerosol performance of the dual targeting formulation were examined. The prophylactic efficacy of the mAb formulation against SARS-CoV-2 was also studied in hamsters following intranasal and pulmonary delivery. In the context of variants with enhanced transmissibility, the protective effects of the dual targeting antibody formulations in treated hamsters cohoused with SARS-CoV-2 Delta variant challenged hamsters were also investigated.

2. Materials and methods

2.1. Materials

Humanised WKS13 mAb was prepared from immunised mice, with the Fc fragment replaced with human IgG1 Fc [manuscript under revision, see supplementary data]. 2-hydroxypropyl-β-cyclodextrin (HPBCD), L-leucine, Brilliant Blue R-250, phosphate-buffered saline (PBS) and sodium phosphate (Na_3PO_4) were purchased from Sigma Aldrich (Saint Louis, USA). Dithiothreitol (DTT), prestained protein ladder (PageRuler™ Plus), Dulbecco's Modified Eagle Medium (DMEM) and foetal bovine serum (FBS) were purchased from Thermo Fisher Scientific (Waltham, MA, USA). All reagents were of analytical grade or higher unless otherwise stated.

2.2. Preparation of dry powder formulation of WKS13 by spray drying

The feed solution was prepared by mixing stock solutions of WKS13 (15 mg/mL in PBS), HPBCD (30 mg/mL in water) and leucine (10 mg/mL in water) to a final solute concentration of 2% (*w/v*) (Table 1). The feed solution was mixed by gentle swirling and loaded into a syringe pump (Legato 210, KD Scientific, MA, USA). All spray dried formulations were prepared using a laboratory scale spray dryer with a high-performance cyclone (Mini Spray Dryer B-290, Büchi Labortechnik AG, Flawil, Switzerland), with aspiration rate at 100% (approximately 35 m^3/h) and inlet temperature of 100 °C (an outlet temperature of 62–64 °C was measured in all formulations). Half of the feed solution was atomised at a feed rate of 0.9 mL/min with a two-fluid nozzle (TFN; Büchi, Switzerland) operated with a nitrogen gas flow rate of 742 L/h. The other half of the feed solution was atomised at a feed rate of 2.5 mL/min with an ultrasonic nozzle (USN; Büchi, Switzerland) controlled at 1.0 W. The spray dried powders produced by the two different nozzles were collected separately and stored in desiccators until further analysis. Blank powder formulations that contained only excipients without mAb were also prepared (Supplementary Table S1). The production yield was defined as the percentage mass of powder collected to the initial total

Table 1
Dry powder formulations of WKS13 mAb produced by spray drying. The mixed formulations were prepared by blending two single formulations at a specific ratio (*w/w*).

		Single formulations			
		C-TFN	C-USN	Cleu-TFN	Cleu-USN
Nozzle		Two-fluid nozzle	Ultrasonic nozzle	Two-fluid nozzle	Ultrasonic nozzle
Composition		WKS13: HPBCD 10: 90 (w/w)		WKS13: HPBCD: Leucine 10: 70: 20 (*w/w*)	
Feed rate (mL/min)		0.9	2.5	0.9	2.5
Mixed formulations (mixing ratio: w/w)	M-C3	3 :	1		
	M-C2	1 :	1		
	M-C1	1 :	3		
	M-Cleu3			3 :	1
	M-Cleu2			1 :	1
	M-Cleu1			1 :	3

solute mass in the feed solution. To prepare dual targeting formulations, spray dried WKS13 powders that were produced with the same feed solution but different nozzle were mixed at different weight ratios using a Turbula® shaker-mixer type T2F (Willy A. Bachofen AG Maschinenfabrik, Basel, Switzerland) (Table 1). A total of 50 mg of powder was weighed into a 50 mL glass vial and subjected to a constant rotational speed of 49 rpm for 10 min [12].

2.3. Morphology study and residual moisture measurement

The morphology of the spray dried WKS13 powder was visualised by scanning electron microscopy (SEM; Hitachi S-4800 N, Tokyo, Japan) at 5 kV. The powders were sprinkled onto black adhesive carbon tape that was pasted on aluminium stubs. Any excess layers of powder were removed by clean air. The stubs were sputter-coated with approximately 13 nm of gold-palladium alloy for 120 s using a sputter coater (Q150R ES Plus, Quorum Technologies, East Sussex, UK). The residual moisture content of the spray dried WKS13 powder was determined by thermogravimetric analysis (TGA). Approximately 3 mg of each powder formulation was heated from ambient temperature to 105 °C at a constant rate of 10 °C/min in a thermogravimetric analyser (TGA 5500, TA Instruments, Newcastle, DE, USA). The residual moisture content was determined by the final weight loss upon heating.

2.4. Particle size distribution and aerosol performance evaluation

The volumetric size distribution of the spray dried WKS13 powders was measured using a HELOS/KR laser diffractometer (Sympatec, Germany) as previously described [12]. In brief, a nasal powder device (Unit Dose System Powder Nasal Spray, Aptar Pharma, France) was filled with 3.0 ± 0.5 mg of powder and manually dispersed. The particle size data are presented as D_{10}, D_{50}, and D_{90}, which represent the equivalent spherical volume diameters at 10%, 50% and 90% cumulative volumes, respectively. Span was calculated as $(D_{90} - D_{10})/D_{50}$. The most representative volumetric particle size distribution of each formulation were plotted for comparison. The aerodynamic size distribution of the spray dried WKS13 powders was evaluated using a Next Generation Impactor (NGI) coupled with a 1 L glass expansion chamber (Copley, Nottingham, UK) as previously described [12]. Briefly, 6 mg of powder was loaded into a nasal powder device (Unit Dose System Powder Disposable Nasal Spray, Aptar Pharma, France) and dispersed at a flow rate of 15 L/min. Ultrapure water was used to rinse and dissolve the powder deposited on all stages of the NGI. The collected samples were filtered through a 0.45-μm membrane filter and the concentration of HPBCD was quantified by an established high-performance liquid chromatography (HPLC) method as previously described [16]. Fifty microlitres of sample was injected into two conjoined Hi-Plex H guard columns (Agilent Technologies, Santa Clara, CA, USA) with ultrapure water as the mobile phase at 65 °C, running at a flow rate of 0.6 mL/min. HPBCD was detected with the refractive index detector (RID) and the peaks were integrated with the Agilent Technologies OpenLab CDS ChemStation Edition (version C.01.06) software. For each powder formulation, dispersions were performed in triplicates. The recovered dose was defined as the total mass of HPBCD quantified on all stages of the NGI. Residual fraction (RF) referred to the fraction of powder that was undispersed and remained in the nasal device. Nasal fraction (NF) was defined as the percentage fraction of powder that had an aerodynamic diameter of over 10.0 μm. Throat fraction (TF) was defined as the percentage of particles with aerodynamic diameter between 5.0 μm and 10.0 μm. Fine particle fraction (FPF) was defined as the percentage fraction of particles with aerodynamic diameter below 5.0 μm. All fractions (RF, NF, TF and FPF) were calculated with respect to the recovered dose.

2.5. Protein content, integrity and monomer measurement

The spray dried WKS13 powders were reconstituted in ultrapure water and the antibody concentration was measured by UV absorbance at 280 nm (Take3™ microvolume plate, BioTek® Instruments, VT, USA). Sodium dodecyl sulfate-polyacrylamide gel electrophoresis (SDS-PAGE) was conducted to examine the molecular weight of mAb before and after the spray drying process. Unformulated WKS13 was included as a control. One set of samples were prepared with SDS at room temperature, the other was reduced with 5 mM dithiothreitol (DTT) and boiled at 95 °C for 5 min in a dry bath. Two micrograms of mAb samples (reduced and non-reduced) were loaded into the wells of 10% acrylamide gels. The electrophoresis system (Mini-PROTEAN® Tetra System, Bio-Rad) was controlled at an applied voltage of 80 V for 40 min, followed by 120 V for 60 min. Once the electrophoresis was completed, the gels were stained in 0.1% *w/v* Coomassie Brilliant blue R-250 for 2 h. The stained gels were destained by washing twice with fresh destaining solution every 2 h and left to destain overnight. The gel with the stained protein bands were imaged using gel documentation system (G:BOX Chemi XR5, Syngene, Cambridge, UK) operated with the Genesys software (version 1.6.9.0, Syngene). To monitor potential protein aggregation, the monomer content of mAb in the formulations were quantified before and after spray drying using size-exclusion chromatography (SEC). Fifty microliters of buffer-reconstituted spray dried WKS13 samples, adjusted to a protein concentration of 200 μg/mL, were injected into a Yarra™ 3 μm SEC-3000 column (Phenomenex®, Torrance, CA, USA) with aqueous Na_3PO_4 as the mobile phase at 25 °C, running at a flow rate of 0.8 mL/min. Using a diode array detector (Agilent Technologies), eluted proteins were detected at 214 nm. The monomer peaks were integrated using Agilent Technologies OpenLab CDS ChemStation Edition (version C.01.03) software and the percentage of monomer content was calculated.

2.6. Animal ethics approval

Male Syrian hamsters (4–6 weeks old) were obtained from the Chinese University of Hong Kong Laboratory Animal Service Centre through the University of Hong Kong (HKU) Centre for Comparative Medicine Research. The experimental procedures were approved by the Committee on the Use of Live Animals in Teaching and Research of HKU (CULATR 6094–22) and were performed according to the standard operating procedures of Biosafety Level 3 animal facilities as previously described [17].

2.7. In vivo prophylactic efficacy of WKS13 formulations against SARS-CoV-2

2.7.1. Single administration of reconstituted liquid of WKS13 formulations through intranasal route

The hamsters were divided into six groups (four hamsters per group). In the first four groups, spray dried powders of WKS13 (C-TFN, C-USN, Cleu-TFN, Cleu-USN) were respectively reconstituted in PBS (5 mg powder in 100 μL PBS, containing 500 μg mAb) and administered dropwise using a pipette to the nostrils of hamsters under anaesthesia by intraperitoneal injection of ketamine (200 mg/kg) and xylazine (10 mg/kg). The other two groups received either an equal volume of PBS (100 μL) *via* intranasal administration (negative control) or an equal amount of unformulated WKS13 (500 μg mAb) *via* intraperitoneal injection (positive control).

2.7.2. Dual administration of WKS13 formulations through intratracheal and intranasal routes

The hamsters were divided into five groups (four hamsters per group). The first group of hamsters received C-TFN powder (2.5 mg, containing 250 μg mAb) through intratracheal administration, followed by intranasal administration of C-USN powder (2.5 mg, containing 250

μg mAb). The second group of hamsters received C-TFN as reconstituted solution (2.5 mg powder in 100 μL PBS, containing 250 μg mAb) through intratracheal administration, followed by intranasal administration of C-USN as reconstituted solution (2.5 mg powder in 100 μL PBS, containing 250 μg mAb). The other two groups received blank powder (C-TFN-B) or PBS through intratracheal administration, followed by intranasal administration of blank powder (C-USN-B) or PBS (negative controls), respectively. The last group received an equal amount of unformulated WKS13 *via* intraperitoneal injection (positive control). During intratracheal administration, powder was dispersed using a dry powder loading device into a guiding cannula that was intubated into the trachea of the hamster as previously described [18]. For intratracheal liquid administration, a high-pressure syringe (Model FMJ-250; PennCentury Inc., Wyndmoor, PA, USA) was filled and aerosolised with the Microsprayer® Aerosolizer (model IA-1C; PennCentury Inc., Wyndmoor, PA, USA) [19]. During intranasal administration, powder was delivered using the dry powder insufflator (PenWu Device for Dry Powder (Mouse), BJ-PW-FM-M; Shanghai BioJane Biological Technology, Shanghai, China) by gentle insertion into the nostril of the hamster [20]. For liquid administration, the reconstituted solution was administered dropwise using a pipette into the nostrils of hamsters under anaesthesia.

2.7.3. SARS-CoV-2 challenge after administration of WKS13 formulations

WKS13 was administered at a dose of 500 μg mAb per animal (equivalent to ~5 mg/kg) in all groups. At 24 h post-administration, the hamsters were intranasally challenged with 10^5 plaque-forming units (p.f.u.) SARS-CoV-2 Delta strain (B.1.617.2) (hCoV-19/Hong Kong/HKU-210804-001/2021; GISAID: EPI_ISL_3221329). All hamster groups were sacrificed for virological and histopathological analyses at four days post-infection (d.p.i.) as previously described [21]. The nasal wash and right lung homogenate were used for the determination of viral burden using quantitative real-time reverse transcriptase-polymerase chain reaction (qRT-PCR) and median tissue culture infectious dose ($TCID_{50}$) assay, while the left lung was used for histopathological analysis and immunofluorescence staining.

2.8. In vivo contact transmission study

The contact transmission studies were performed as previously reported [22]. The hamsters were divided into three groups (each group includes 3 repeats of donor and receipt hamster combination). The first recipient group was administered with C-TFN powder (2.5 mg) intratracheally, followed by intranasal administration of C-USN powder (2.5 mg). The second recipient group was administered with blank powder intratracheally, followed by intranasal administration of blank powder (negative control). The third recipient group received unformulated WKS13 intraperitoneally (positive control). The three donor groups of hamsters were intranasally challenged with SARS-CoV-2 Delta variant at 0 d.p.i. After 24 h, each virus-challenged donor hamster was transferred to a new cage with one naïve recipient hamster as a close contact. The hamsters were co-housed for 4 h before transferal to separate new cages. The donor and recipient hamsters were sacrificed at 4 d.p.i. and 4 days post-treatment, respectively, for viral load quantification using qRT-PCR method.

2.9. Determination of viral load by qRT-PCR

Lung tissues were homogenised and extracted for total RNA with RNeasy Mini RNA Extraction Kit (Qiagen, Hilden, Germany). Nasal wash samples collected into 400 μL of viral transporting medium were extracted for total RNA using QIAamp Viral RNA Mini Kit (Qiagen, Hilden, Germany). One step qRT-PCR was performed for the detection of the copies of SARS-CoV-2 virus RdRp gene using QuantiNova Probe RT-PCR kit (Qiagen, Hilden, Germany) on LightCycler 480 system (Roche) as previously described [23]. Primers and probes were listed as follow - SARS-CoV-2 RdRp, forward: 5' CGCATACAGTCTTRCAGGCT 3′; reverse: 5' GTGTGATGTTGAWATGACATGGTC 3′; probe (5′ to 3′): FAM-TTAAGATGTGGTGCTTGCATACGTAGAC-lABkFQ. β-actin,Forward: 5' ATGGCCAGGTCATCACCATTG 3′; Reverse: 5' CAGGAAGGAAGGCTG-GAAAAG 3′; Probe (5′ to 3′): Cy5-AGCGGTTCCGTTGCCCTGAG-IABkFQ.

2.10. Median tissue culture infectious dose ($TCID_{50}$) assay

Infectious virus titres in the lung and nasal wash were determined by $TCID_{50}$ assay in VeroE6 cells as previously described [24,25]. The lung and nasal wash samples were homogenised in culture medium, and the supernatant was collected by centrifugation. The samples were diluted serially at 10-folds with culture medium and inoculated into confluent VeroE6 monolayer. After virus absorption at 37 °C for 1 h, the inoculum was removed; cells were washed and returned to culture at 37 °C in 5% CO_2 for 72 h. Cytopathic effects were observed. $TCID_{50}$, defined as the dilution of virus required to infect 50% of a cell culture, was calculated using Spearman-Karber method.

2.11. Histology and immunofluorescence staining

Fixed hamster lung tissues were processed, embedded, and cut to prepare 5 mm thick tissue sections on glass slides. Before staining, the slides were dewaxed with xylene and serially decreased ethanol concentrations (100%, 95%, 70%). The tissue slides were stained with Gill's haematoxyline and eosin (H&E) (Thermo Fisher Scientific, Waltham, MA, USA) as previously described [26]. Viral antigens were stained by immunofluorescences with specific antibodies: rabbit anti-SARS-CoV-2 nucleocapsid (N) antibody [22].

2.12. Statistical analysis

All statistical analyses were conducted with GraphPad Prism (GraphPad Software, La Jolla, CA, USA). The sample size (n) was indicated in the text or figure captions for each experiment. A significance level of $p < 0.05$ was considered statistically significant throughout this study.

3. Results

3.1. Physicochemical properties of spray dried WKS13 mAb powder formulations

WKS13 dry powders were produced by spray drying using TFN or USN to obtain particles with suitable size range for lung and nasal deposition, respectively. The formulations were prepared either with HPBCD as the sole excipient (C-TFN and C-USN), or with the addition of leucine (Cleu-TFN and Cleu-USN). Powders prepared with TFN had a higher production yield (89.6 to 93.0%) compared to those prepared with the USN (61.8 to 64.1%) (Table 2), possibly because the system was more efficient in capturing small particles. The measured mAb contents

Table 2
The production yield, measured mAb contents and residual moisture content of the spray dried powder formulations of WKS13. Data are presented as mean ± standard deviation ($n = 3$).

Formulation	C-TFN	C-USN	Cleu-TFN	Cleu-USN
Production yield (% *w*/w)	89.6	61.8	93.0	64.1
mAb content (% w/w)	8.9 ± 0.5	8.3 ± 0.4	8.1 ± 0.4	8.4 ± 0.3
Residual moisture [#] (% w/w)	3.6 ± 0.5	2.9 ± 0.2	2.3 ± 0.1	2.0 ± 0.2

[#] No significant difference between TFN and USN formulations prepared with the same feed solution ($p > 0.05$).

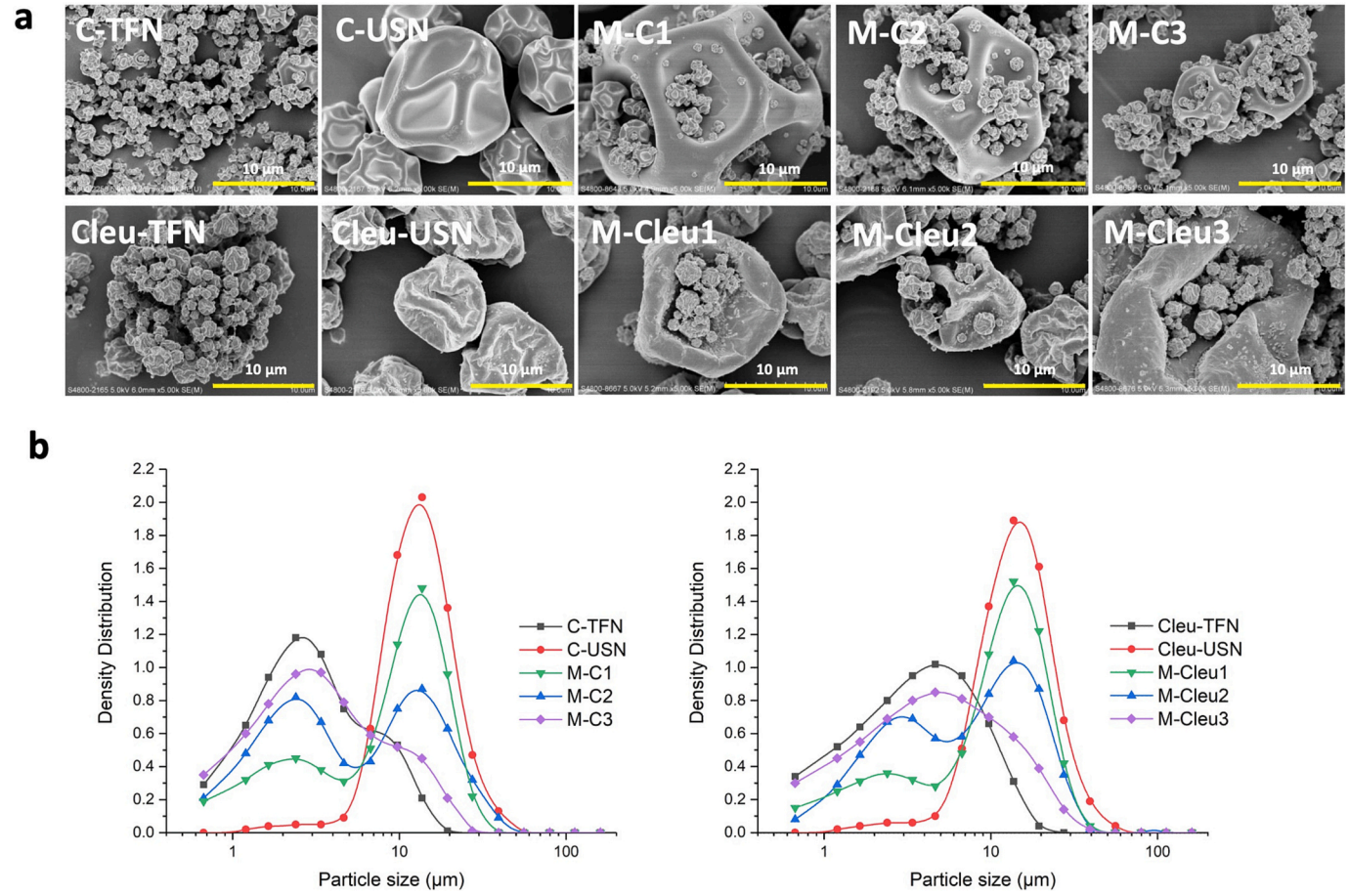

Fig. 1. Morphology and particle size distribution of the spray dried WKS13 formulations. (a) Scanning electron microscope (SEM) images at 5.0 k magnification (scale bar = 10 µm). (b) Incremental particle size distribution measured by laser diffraction. The most representative volumetric particle size distribution data of each formulation were plotted for comparison.

in all formulations were above 8% *w*/w (Table 2). All powder formulations demonstrated low levels of residual moisture (< 4% *w*/w) after spray drying) (Table 2), with leucine-containing formulations exhibiting a lower moisture content than their leucine-free counterparts ($p < 0.05$). However, there was no significant difference in residual moisture content between formulations prepared with the same composition but different atomisation nozzle (TFN *vs.* USN, $p > 0.05$). All spray dried powder formulations showed rapid dissolution profile that allows immediate release of WKS13 (Supplementary Fig. S1).

The morphology of the spray dried WKS13 powders was visualised by SEM (Fig. 1a). The particles exhibited irregular indentations in the exterior surface, forming a shrivelled appearance. Those produced with HPBCD as the sole excipient (C-TFN and C-USN) had smoother exterior surfaces and consistent shapes and sizes, as compared to particles produced with the addition of leucine (Cleu-TFN and Cleu-USN) which had coarser surfaces with wrinkled texture. All formulations exhibited a relatively uniform size distribution. Particles produced with the TFN were visibly smaller (<5 µm) than the particles produced with the USN (>10 µm). Upon mixing, a blend of small and large particles can be clearly observed, with the smaller particles loosely scattered around the surface of the larger particles. When mixed at different mixing ratios, the size distribution of the particles corresponded to the proportion of single formulations present in the mixed formulation. Large particles (>10 µm) were the dominant species when there was a high proportion of C-TFN or Cleu-TFN, while small particles (< 5 µm) became more prominent when the proportion of C-USN or Cleu-USN increased. The volumetric particle size distribution was measured by laser diffraction after the powders were dispersed from a nasal powder device. The data are presented as incremental size distribution (Fig. 1b) and equivalent spherical volume diameters at 10%, 50% and 90% cumulative volume (Supplementary Table S2). When particles were prepared with TFN, the particle size was larger when leucine was present in the formulation. Consistent with the SEM images, particles produced with the USN had a larger median size as compared to their TFN counterpart. A bimodal particle size distribution can be distinctly observed when mixed at a 1:1 *w*/w ratio in M-C2 and M-Cleu2 formulations. When the proportion of one formulation increased in the mixed formulation, the peak corresponding to the particle size of that formulation increased accordingly until a unimodal distribution is established.

3.2. Aerosol properties of spray dried WKS13 mAb powder formulations

For a dual targeting formulation, specific ranges of aerodynamic diameter are required to enable efficient deposition at intended sites along the respiratory tract. Particles with aerodynamic diameter >10 µm tend to be deposited in the nasal cavity while particles between 1 and 5 µm tend to deposit in the lower airways. The deposition fractions obtained from the NGI are presented as RF, NF, TF and FPF, which correspond to the powder collected from the nasal device, expansion chamber (representing nasal deposition), throat and NGI collection plates (fraction of particles <5 µm representing lung deposition), respectively (Fig. 2a & b). All formulations were effectively emitted from the nasal device with minimal retention (RF < 3%). Formulations prepared with the USN (C-USN and Cleu-USN) demonstrated high NF (both over 95%) and low FPF (both below 1%), indicating that these powder formulations were almost exclusively deposited in the nasal

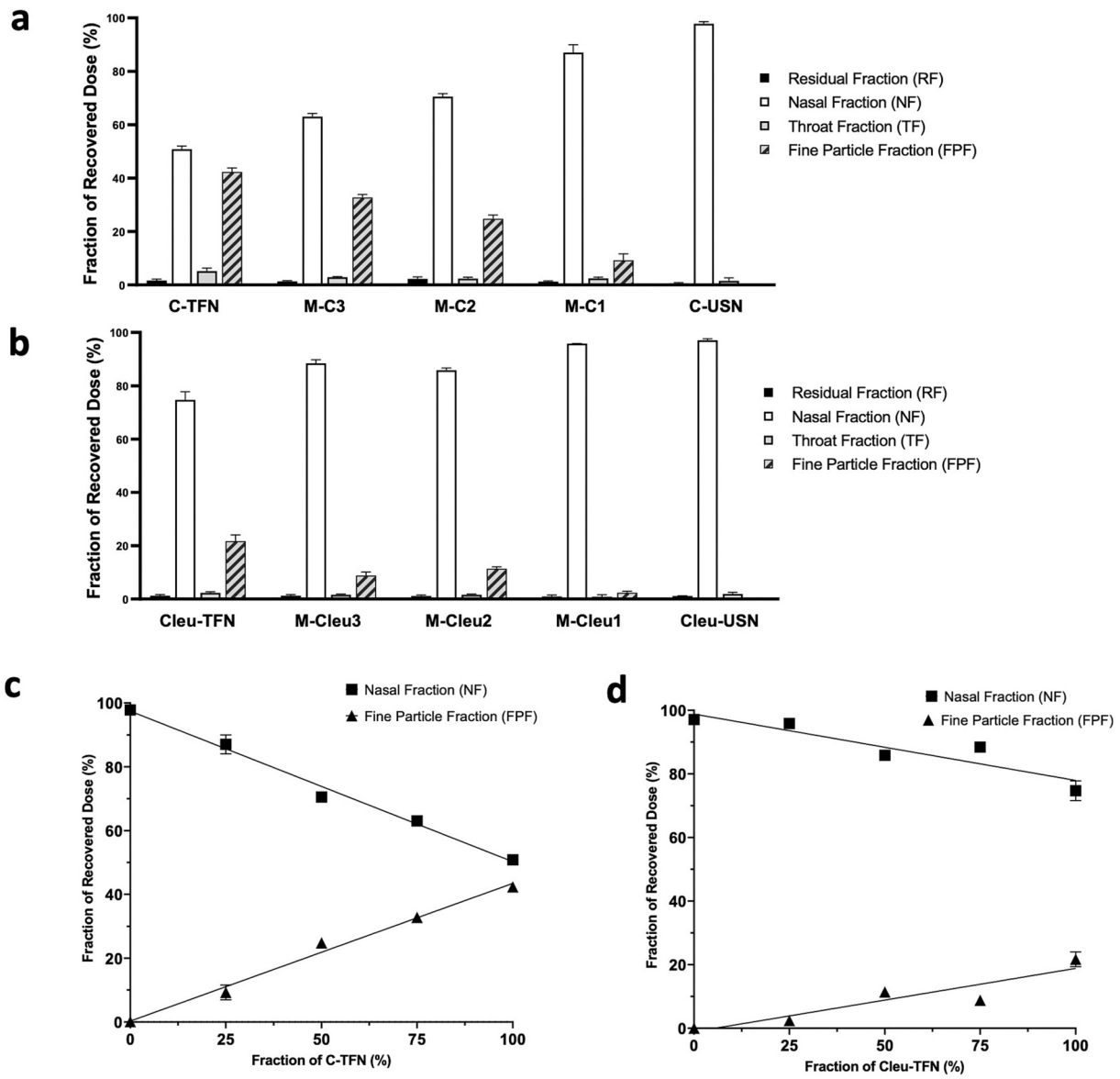

Fig. 2. Aerosol performance of the spray dried WKS13 formulations. (a) M-C powders and (b) M-Cleu powders mixed at different mixing ratios and dispersed with nasal device. The mixed formulations were evaluated using the Next Generation Impactor (NGI) coupled with 1 L glass expansion chamber, operated at 15 L/min. Residual fraction (RF), nasal fraction (NF), throat fraction (TF) and fine particle fraction (FPF) were expressed with respect to the recovered dose. Linear regression of NF and FPF were plotted against fraction of (c) C-TFN and (d) Cleu-TFN in the formulation. Data are presented as mean ± standard deviation ($n = 3$).

cavity. In comparison, formulations prepared with TFN (C-TFN and Cleu-TFN) exhibited higher FPF than their USN counterparts, demonstrating significant lung deposition. Comparing between the leucine-free and leucine-containing formulations, while there was no observable difference in the deposition profile between C-USN and Cleu-USN, the FPF of C-TFN (~42%) was much higher than that of Cleu-TFN (~22%). Overall, the deposition profile of each single formulation matched with its intended deposition site.

To achieve dual deposition in both the nasal cavity and lower airways, TFN and USN formulations were mixed at a range of mixing ratios. At 1:1 mixing ratio, dual deposition was observed in both M-C2 and M-Cleu2, with NF:FPF ratio of 70:25 and 86:11, respectively. As the mixing ratio was further varied, the ratio of NF:FPF followed a linear trend (Fig. 2c & d). The NF:FPF ratio for the M-C formulations exhibited a wider range from 87:10 (M-C1) to 63:33 (M-C3) as compared to the M-Cleu formulations, with a narrow range from 96:3 (M-Cleu1) to 88:9 (M-Cleu3). This trend is due to the low FPF of Cleu-TFN when dispersed from a nasal device. The M-C formulations, with HPBCD as the sole excipient, are hence superior to M-Cleu formulations as the former offer a wider range of NF:FPF for customisable dual targeting delivery by intranasal administration. Conventionally, localised drug delivery to the respiratory tract is delivered through orally inhaled devices such as handheld dry powder inhalers. When dispersed with the Osmohale®, the presence of leucine in Cleu-TFN improved the aerosol performance (EF 73%, FPF 52%) compared to C-TFN (EF 49%, FPF 34%) (Supplementary Table S3). Overall, M-C formulations with HPBCD as the sole excipient demonstrate favourable dual targeting properties for customisable and efficient powder deposition in both the upper and lower airways which are the target sites of respiratory viral infection.

3.3. *Structural integrity of WKS13 mAb in spray dried powder formulations*

To determine the structural integrity of WKS13 mAb, gel electrophoresis was conducted on the mAb samples before and after spray drying (Fig. 3a). The SDS-PAGE images of the non-reduced samples were

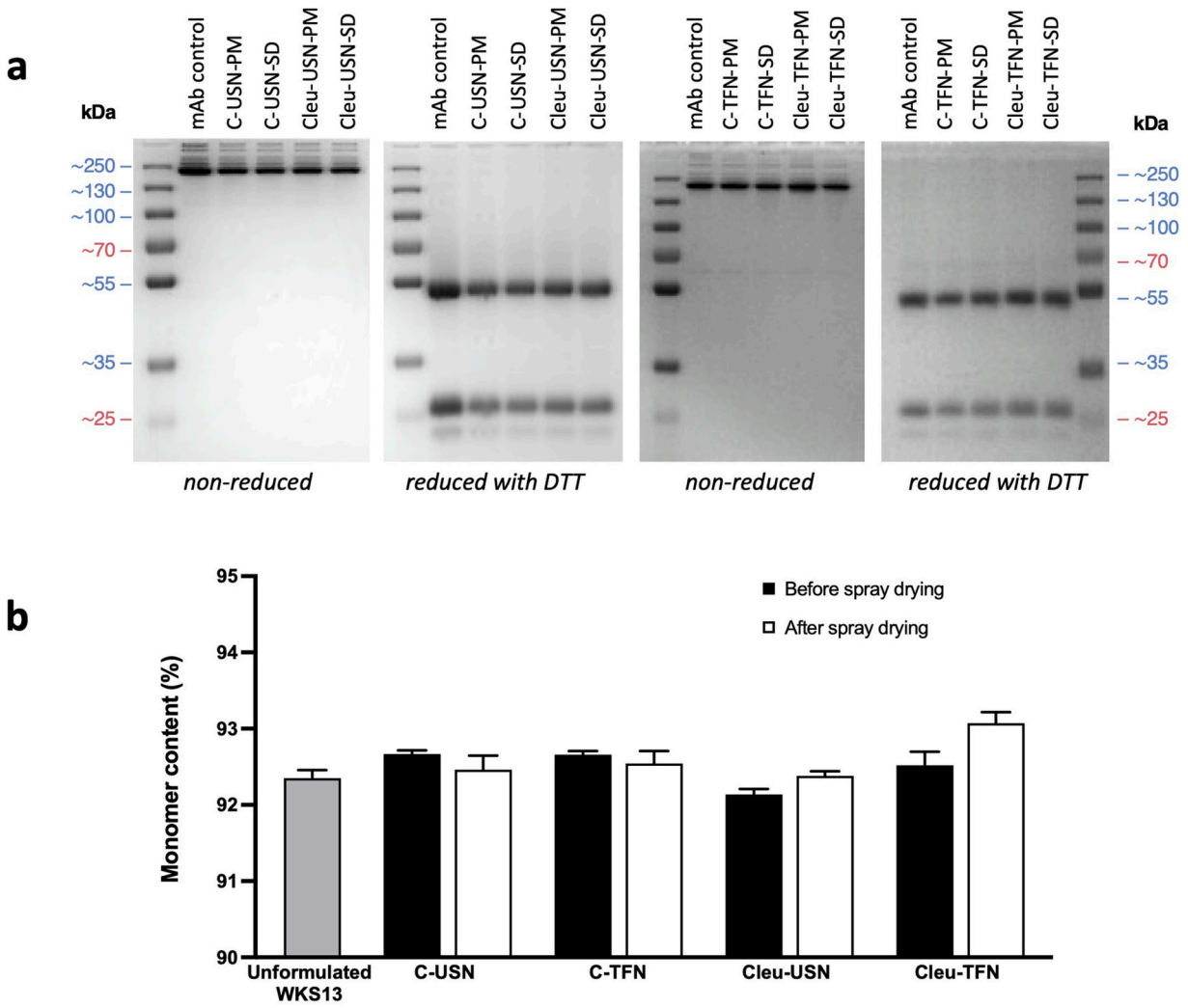

Fig. 3. Integrity of WKS13 in spray dried powder formulations. (a) SDS-PAGE images of WKS13 formulations before (PM) and after spray drying (SD), non-reduced and reduced with dithiothreitol (DTT). (b) Monomer content of WKS13 formulations before and after spray drying. Unformulated WKS13 was used as mAb control for comparison. Data are presented as mean ± standard deviation ($n = 3$).

similar to the unprocessed mAb, showing bands around 150 kDa and no sign of low molecular weight fragments. In the reduced samples, bands at 50 and 25 kDa bands are observed. These low molecular weight bands correspond to the heavy and light chains of the antibody after cleavage of disulfide bonds in the reduced samples. No observable changes in the molecular weight of the mAb before and after spray drying were detected, suggesting that the integrity of WKS13 in the powder samples were preserved. The mAb monomer content was also quantified before and after spray drying (Fig. 3b). The monomer content of all spray dried WKS13 formulations were similar to that of the unformulated mAb or feed solution without being subject to spray drying. No sign of mAb aggregation was observed. The neutralisation activity of WKS13 in the powder formulations was also analysed by incubation with live virus. The antibodies retained their neutralisation activity after spray drying (Supplementary Table S4).

3.4. *In vivo* neutralisation activity of WKS13 formulations against SARS-CoV-2

Prophylactic efficacy of the WKS13 formulations were evaluated by administering the mAb to hamsters 24 h prior to viral challenge, and the lung tissue and nasal wash were collected at 4 d.p.i. (Fig. 4a). To investigate whether WKS13 could retain its *in vivo* neutralisation activity after formulation by spray drying, the spray dried WKS13 powders were first reconstituted in PBS and administered intranasally as solution. The viral loads in the lung tissues of hamsters receiving the WKS13 formulations were significantly lower than that of PBS-treated hamsters ($p < 0.05$), and the results were comparable to the unformulated WKS13 mAb administered intraperitoneally (Fig. 4b). There was no significant difference among the four spray dried WKS13 formulations, or with the unformulated WKS13. However, the effect on viral loads in the nasal wash was less impressive (Fig. 4c). Only the groups received reconstituted C-USN formulation intranasally and unformulated WKS-13 intraperitoneally displayed a significantly lower viral load as compared to the PBS control group ($p < 0.05$). It is speculated that the liquid formulations failed to retain in the nasal cavity, leading to poor local viral neutralisation by the mAb. Nonetheless, $TCID_{50}$ were also measured to determine virus infectivity in the lung (Fig. 4d) and nasal (Fig. 4e) samples. Compared to the PBS control group, the infectious viral titers were significantly lower in both the lung and nasal wash samples in the groups receiving reconstituted WKS13 powders and intraperitoneal unformulated WKS13 ($p < 0.05$).

Next, C-TFN and C-USN were chosen for dual targeting administration due to the wider customisable range of aerosol deposition profile. The hamsters were first administered intratracheally with C-TFN, and subsequently administered intranasally with C-USN (Fig. 5a). The formulations were administered either as dry powder or reconstituted solution. The resultant viral load and $TCID_{50}$ were quantified in the lung

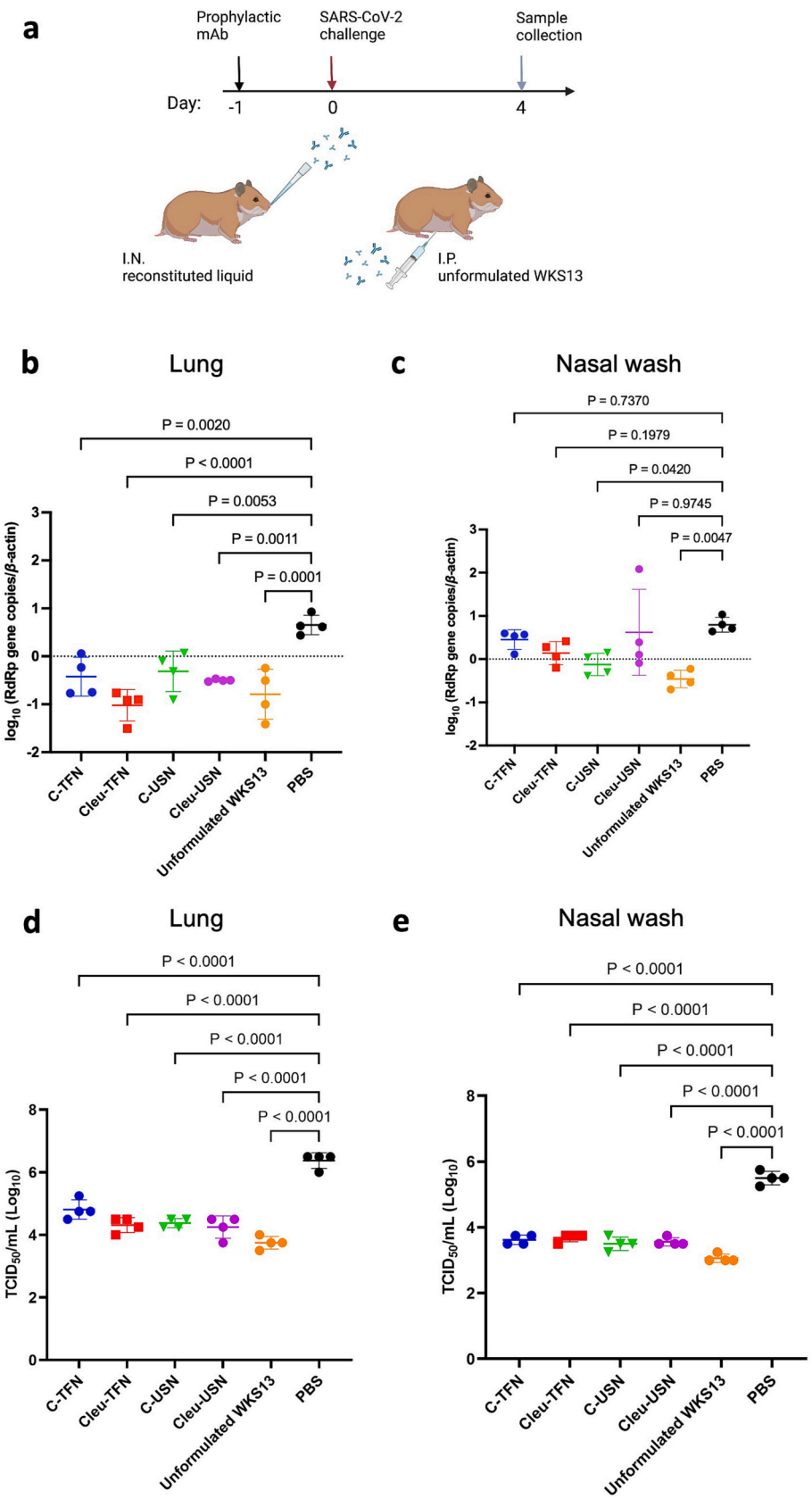

Fig. 4. *In vivo* prophylactic efficacy of reconstituted WKS13 formulations against SARS-CoV-2 Delta variant. (a) Scheme of the prophylactic efficacy - intranasal (I.N.) administration of WKS13 mAb formulations (C-TFN, Cleu-TFN, C-USN and Cleu-USN) as reconstituted liquid, with I.N. administration of PBS or intraperitoneal (I.P.) injection of unformulated WKS13 as controls. Viral loads in the (b) lung tissues and (c) nasal wash were determined by qRT-PCR at 4 days post-infection. Infectious viral titer was determined by $TCID_{50}$ assay in VeroE6 cells for the (d) lung tissues and (e) nasal wash. One-way ANOVA was used for statistical analysis. Data are presented as mean ± standard deviation ($n = 4$).

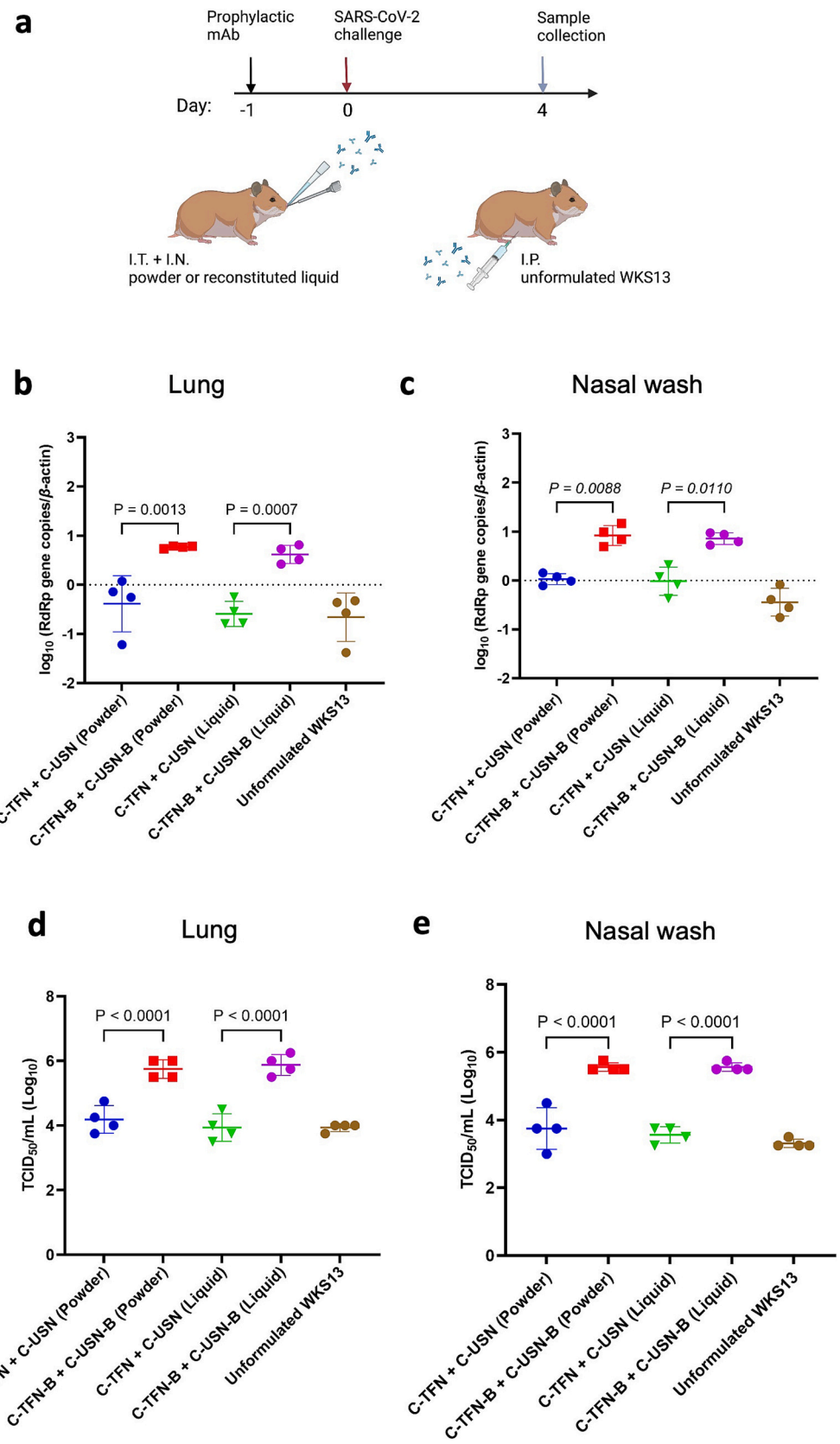

Fig. 5. *In vivo* prophylactic efficacy of dual administration of WKS13 formulations against SARS-CoV-2 Delta variant. (a) Scheme of the prophylactic efficacy study - intratracheal (I.T.) administration of C-TFN and intranasal (I.N.) administration of C-USN as dry powder or reconstituted liquid, with the administration of corresponding blank formulations or intraperitoneal (I.P.) injection of unformulated WKS13 as controls. Viral loads in the (b) lung tissues and (c) nasal wash were determined by qRT-PCR at 4 days post-infection. Infectious viral titer was determined by $TCID_{50}$ assay in VeroE6 cells for the (d) lung tissues and (e) nasal wash. One-way ANOVA was used for statistical analysis. Data are presented as mean ± standard deviation (n = 4). C-TFN-B and C-USN-B indicates blank control of C-TFN and C-USN, respectively.

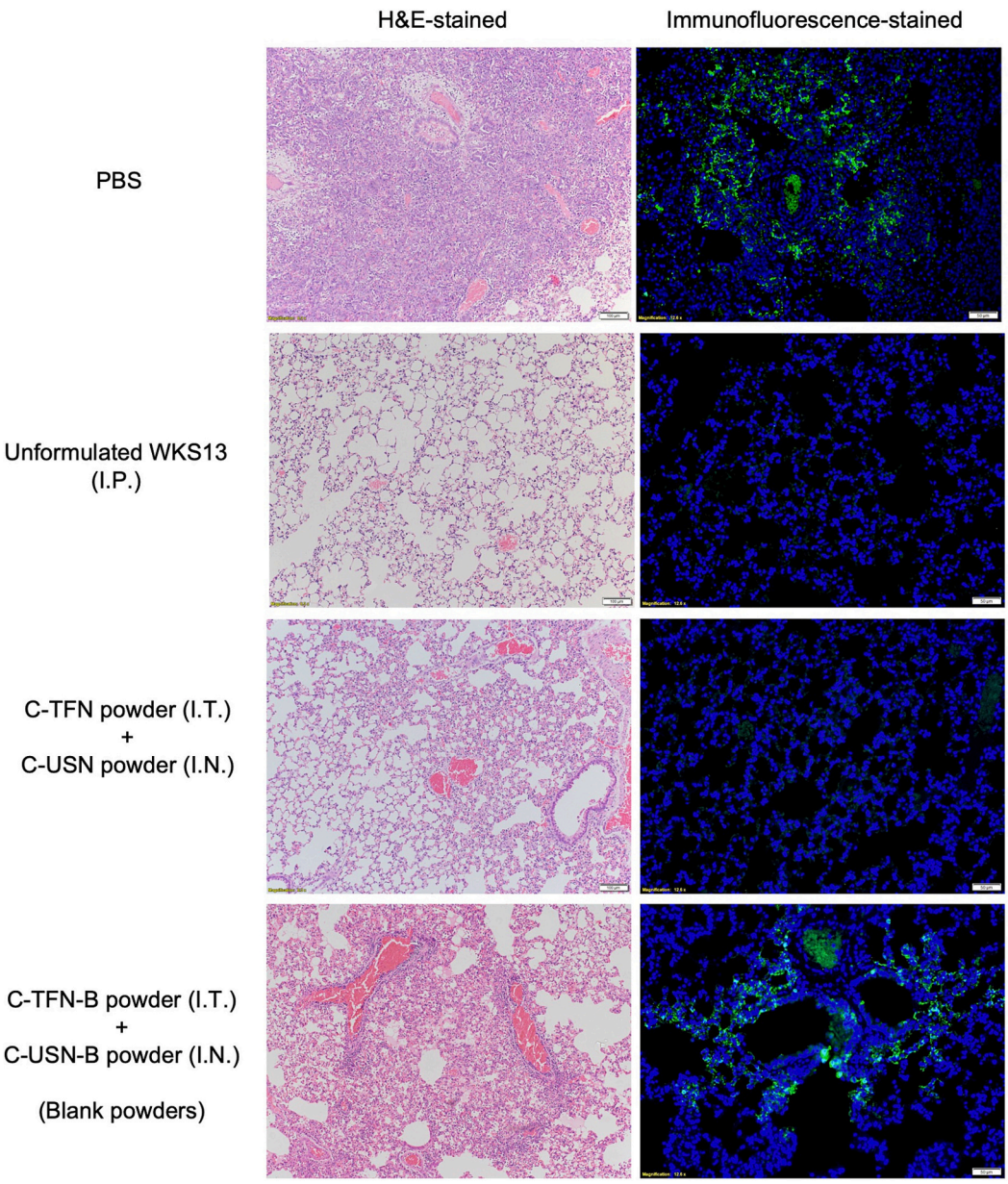

Fig. 6. The histopathological changes and virus replication in the lung tissues of hamsters infected with SARS-CoV-2 Delta variant. The hamsters either received PBS intranasally (I.N.); unformulated WKS13 intraperitoneally (I.P.); C-TFN powder intratracheally (I.T.) and C-USN powder intranasally (I.N.); or C-TFN-B (blank) powder I.T. and C-USN-B (blank) I.N. The lung tissues were harvested at 4 days post-infection. Representative images of H&E stained lung tissue sections (scale bar 100 μm) and immunofluorescence-stained lung tissue sections (scale bar 50 μm) with viral nucleocapsid protein detected by specific antibody (green) and cell nuclei stained by DAPI (blue). (For interpretation of the references to colour in this figure legend, the reader is referred to the web version of this article.)

tissues (Fig. 5b and d) and nasal wash (Fig. 5c and e) of the hamsters, respectively. Regardless of whether powder or liquid form was given, dual administration of C-TFN and C-USN resulted in significantly lower viral load in the lung tissues and nasal wash of hamsters as compared to the control group that received blank formulations ($p < 0.05$). The reduction in viral load were comparable to those receiving unformulated WKS13 mAb intraperitoneally, suggesting that the *in vivo* neutralisation activity of WKS13 was successfully preserved after spray drying. Histopathological examination of H&E stained lung tissues (Fig. 6) revealed alveolar damage and interstitial inflammatory infiltration when hamsters were treated with PBS or blank powders. In contrast, the alveolar damage and interstitial infiltration were alleviated substantially in the lung tissues of hamsters treated with unformulated WKS13 intraperitoneally or dual administration of C-TFN intratracheally and C-USN intranasally. Consistent with the viral loads detected in the lung tissues, the images of immunofluorescence-stained lung tissues (Fig. 6) showed high level of viral nucleocapsid antigen in hamsters treated with PBS or blank powders but not in animals that received WKS13, either as unformulated mAb or dual administration the C-TFN and C-USN powder formulations. In addition, there were no significant changes in body weight over time for animals receiving WKS13 formulations (Supplementary Table S5 and S6). Collectively, these results indicate that dual delivery of mAb powders offered safe and effective antiviral protection against SARS-CoV-2 Delta variant infection in a prophylactic setting.

3.5. *In vivo contact transmission study of dual targeting WKS13 formulation against SARS-CoV-2*

Currently, Syrian hamsters are the only rodent model in which airborne transmission can easily be tested. In this study, the

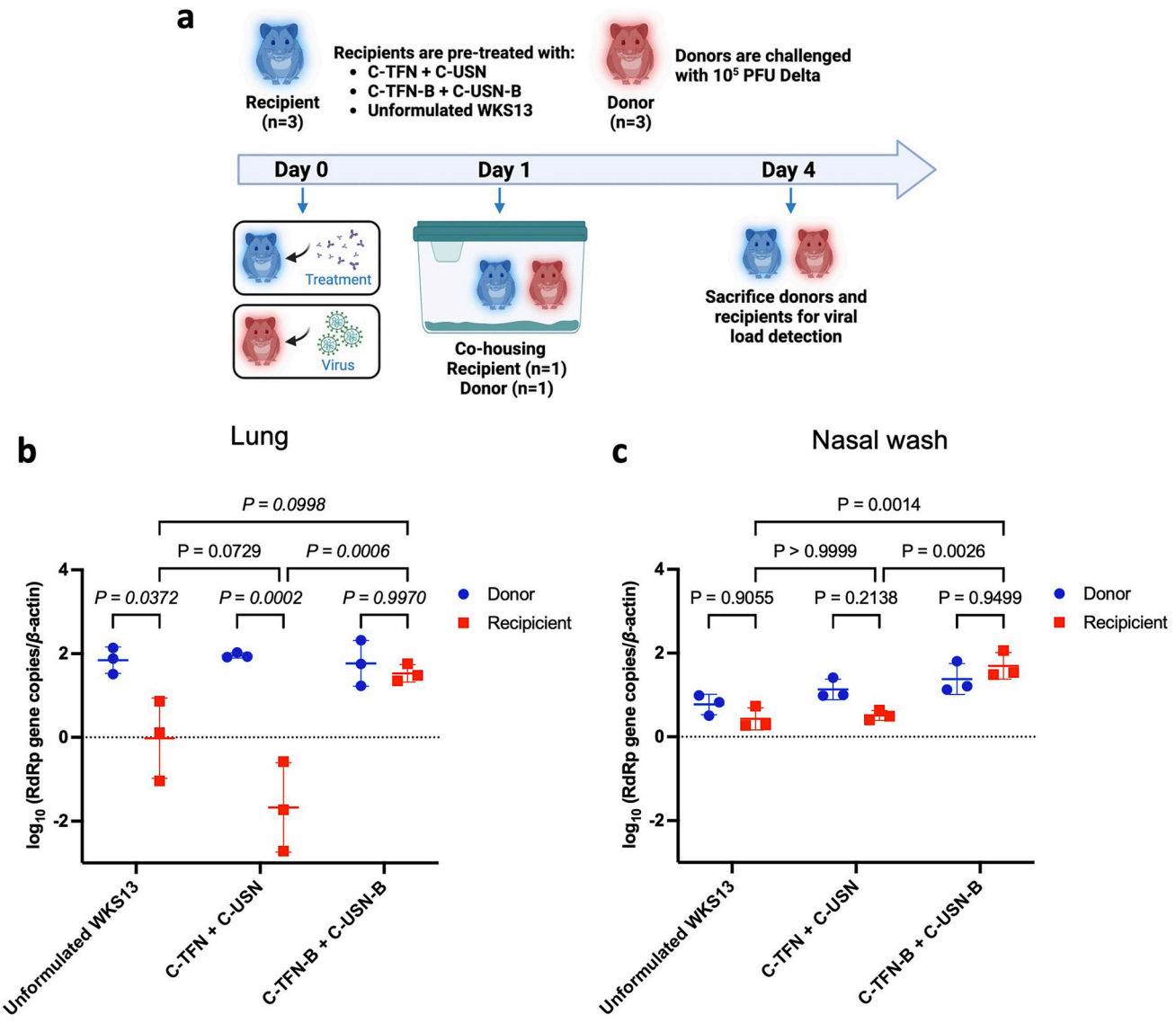

Fig. 7. *In vivo* contact transmission study of SARS-CoV-2 Delta strain. (a) Scheme of the contact transmission study - the donors were challenged with SARS-CoV-2 Delta variant; the recipients were pre-treated with dual administration of C-TFN/C-USN powder formulations or blank formulations through intratracheal and intranasal route, or unformulated WKS13 by intraperitoneal injection on the same day. Co-housing between donor and receipt hamsters were performed on 1 day post-infection for 4 h before transferal to single housing. Viral loads in the (b) lung tissues and (c) nasal wash of all hamsters were determined by qRT-PCR after 4 days of post-infection or post-treatment. Two-way ANOVA was used for statistical analysis. Data are presented as mean ± standard deviation ($n = 3$).

transmissibility of SARS-CoV-2 Delta variant was evaluated by cohousing WKS13-treated hamsters (recipient) with those challenged with the virus (donor) (Fig. 7a). At the same 0 d.p.i., recipient hamsters were treated with WKS13 whereas donor hamsters were challenged with SARS-CoV-2. At 1 d.p.i., when significant virus shielding become detectable from the donor hamsters, each animal was co-housed with the other recipient hamster to enable close contact. Viral loads in the lungs and nasal wash were quantified at 4 d.p.i., and the results were compared between the donor and recipient groups as a reflection of virus transmission. The pre-treatment with dual administration of C-TFN powder (to the lung) and C-USN powder (to the nasal cavity) offered protection to animals from the viruses (Fig. 7b), as indicated by the significantly reduced viral load in the lung tissues in the recipient group ($p < 0.05$), while the administration of blank formulations did not achieve the same effect, indicating that transmission of virus occurred when the animals did not receive WKS13 mAb. The viral load in the lungs of animals treated with dual administration of mAb formulations was on average 100-fold lower than those treated with intraperitoneal injection of unformulated mAb although there was no significant difference between the two groups ($p = 0.0729$), indicating localised aerosol delivery to the lungs enabled more efficient blockage of viral transmission. In terms of nasal wash, both recipient groups that received mAb, either as unformulated WKS13 ($p = 0.0014$) or dual administration of WKS13 formulations ($p = 0.0026$), displayed a significantly lower viral load as compared to the recipient group that received blank formulations (Fig. 7c). Overall, the transmission study suggested that dual administration WKS13 formulations offer considerable benefits by reducing the viral loads in both upper and lower respiratory tracts of recipient animals, which may reduce the risk of severe infection.

4. Discussion

Neutralising mAb is invaluable in combating respiratory viral infections, with several mAbs already approved for prophylaxis or treatment of COVID-19 [27–29]. However, there are limitations in the use neutralising mAb against viruses. For instance, mutations in the SARS-CoV-2 spike protein, which is the major target of neutralising mAbs, enable viruses to escape neutralisation, as shown in the resistance of

Omicron subvariants to mAb [30]. There are several strategies to improve the efficacy of neutralising mAb. One strategy is to design mAb with broad-spectrum activity, such as the WKS13 used in this study. Another strategy is to improve delivery efficiency [31]. We propose to adopt a dual targeting approach, the concept of which entails the delivery of a therapeutic agent directly to both the nasal cavity and lower lung region simultaneously for enhanced therapeutic efficacy at the two major sites of infection. Since the site of deposition in the airways is largely dependent on particle size, dual targeting mAb formulations could be obtained by blending mAb powder of two different particle size range to achieve deposition in the intended regions of the respiratory tract, *i.e.*, the nasal cavity and lower airways.

One of the major challenges in developing dry powder aerosol of mAb is to preserve protein integrity while achieving good powder dispersibility and aerosolisation for effective deposition in the respiratory tract. Spray drying is a particle engineering technique that involves flash drying of atomised droplets at an elevated temperature. Although this drying technology is commonly utilised to produce inhalable powders of vulnerable biological molecules [19,32,33], the drying process using high temperature and atomisation nozzles inevitably subjects mAb to shear, interfacial and thermal stresses that may contribute to the instability of proteins, causing fragmentation and aggregation. HPBCD, which is a cyclodextrin derivative, was chosen in this study to be the excipient because of its protein stabilising property [14,34]. It has been suggested that cyclodextrin can inhibit protein aggregation by binding to the exposed hydrophobic residues on proteins. It also exhibits non-ionic surfactant effect by displacing proteins from the air-liquid interface during atomisation, thereby protecting them from denaturation. Apart from the choice of excipient in the formulation, the process condition is also crucial when formulating the heat-labile mAb. The employment of HPBCD as stabiliser coupled with the relatively mild spray drying condition (inlet temperature of 100 °C; outlet temperature below 65 °C) successfully preserved the mAb integrity with no evidence of fragmentation or aggregation, and the drying was complete with a low residual moisture content of below 4% across all spray dried WKS13 formulations. Most importantly, all WKS13 formulations remained biologically active, as shown in the *in vitro* live virus neutralisation antibody assay and the *in vivo* prophylactic efficacy study. Furthermore, WKS13 was instantaneously released upon powder dissolution in all formulations, thereby providing rapid onset of action.

Leucine is commonly used in inhaled dry powder aerosol formulation to improve powder dispersibility [15,35,36]. The incorporation of leucine in the formulation has led to increased hydrophobicity and surface roughness of spray-dried particles, thereby promoting powder de-aggregation. As expected, Cleu-TFN had a higher FPF than C-TFN when the powders were dispersed from an oral inhaler. However, its role as dispersion enhancer was not reflected when the powders were dispersed from a nasal device. The FPF of Cleu-TFN was almost half of C-TFN. As the nasal device used in this study is an active device in which the powders are dispersed by compressed air generated by a pump-like mechanism [37], the role of leucine was diminished as all formulations (with or without leucine) were extremely effective in emitting from the nasal device. On the contrary, Cleu-TFN powders displayed a much larger particle size, with the median diameter almost double to that of C-TFN. This observation could be explained by the low aqueous solubility of leucine. The rapid evaporation of solvent during spray drying led to crystallisation of leucine on the droplet surface, resulting in the formation of large and hollow particles [38]. The FPF of Cleu-TFN was barely over 20%, only a small proportion of powder could reach the lower airways following dispersion from a nasal device. An ideal dual targeting formulation would contain a blend of two powder species, one efficient in depositing in the nasal cavity while the other efficient in depositing in the lung. This would allow a wide range of customisable deposition profiles to be created by mixing the two at an appropriate ratio. Given the poor lung deposition of the Cleu formulations following dispersion from a nasal device, the C-TFN and C-USN pair was identified to be more suitable for use in the dual targeting formulation.

Due to the substantial anatomical and physiological differences between rodents and humans, the dual deposition profile of C-TFN/C-USN blends (*i.e.* the M-C formulations), which were designed for human use, was not examined in animals. Instead, C-TFN and C-USN were administered separately to the lung and nasal cavity of hamsters, respectively, to evaluate their neutralisation effect. The *in vivo* prophylactic efficacy of WKS13 was successfully demonstrated with this dual administration approach. Significantly lower viral loads in both the upper and lower respiratory tract was observed after direct viral infection and indirect transmission from infected hamsters, suggesting lowered risk of severe infection and transmissibility. Previous studies that investigated local delivery of neutralising mAbs have been focused on administration through nebulisation or intranasal instillation of liquid formulation [29]. The direct administration of neutralising mAb in dry powder form through the pulmonary and/or intranasal route has yet to be reported. Although the antiviral effect was not superior to systemic administration of the unformulated WKS13 mAb in the current study, the dual targeting approach using nasal powder to deliver neutralising mAb offers several unique advantages. Formulation of mAb as dry powder can improve protein stability with extended shelf-life while avoiding cold-chain logistics. Moreover, it is non-invasive, portable, with the possibility of self-administration for use in outpatients. These attributes are particularly useful when a rapid mass distribution of neutralising mAb is required during an early stage of a disease outbreak to prevent the transmission and progression of a highly contagious infectious disease.

One interesting observation is that the WKS13 formulations appeared to be more effective in neutralising viruses in the lung than in the nasal cavity of hamsters. This could be related to both the mechanism of action of mAb against the viruses and the design of the powder formulations. SARS-CoV-2 enters the host cells *via* the angiotensin-converting enzyme 2 (ACE2) receptors and WKS13 blocks viral entry to the hosts by binding to the ACE2 RBD of SARS-CoV-2 spike protein. In human, ACE2 receptors are found to be most abundantly expressed in the nasal cavity, with decreasing expression from the upper to lower respiratory tract [39,40]. While the expression of ACE2 receptors in hamsters is not clearly understood, it is possible that the neutralising effect can be more prominent in the lower airways than in the nasal cavity due to the different expression levels of ACE receptors at these two sites. In the current study, an equal dose of WKS13 was applied to the lung and nasal cavity when the dual targeting approach was employed. To maximise the efficiency of WKS13, the dose of mAb between the two target sites could be adjusted by manipulating the ratio of the dual powder blend. In addition, neutralising mAb must be present at the airway epithelium to interfere with the virus-host interaction before viral entry occurs. The rate of mucociliary clearance in the nasal cavity is higher than that in the lower airways due to the higher population of ciliated cells [41]. As a result, particles deposited in the nasal cavity tend to be removed more quickly from the airways. Formulation strategy by incorporating mucoadhesive agents such as chitosan and methylcellulose derivatives [42] into the nasal fraction could be considered to maximise the nasal residence time of mAb for prolonged neutralisation activity.

5. Conclusions

Overall, dual targeting nasal powder formulation is a promising strategy for delivering neutralising mAb to the respiratory tract as a prophylactic measure against respiratory viral infections. This is particularly important in a ‘post-pandemic’ era, whereby severe cases have dramatically decreased and prophylactic measures are becoming increasingly critical to reduce virus transmission to protect high-risks populations and to reduce socioeconomic loss due to absence from work. With the use of spray drying technique and HPBCD as stabiliser excipient, dry powders of WKS13 with preserved structural integrity and biological activity that was comparable to the unformulated antibody

were successfully produced. A dual targeting formulation with customisable aerosol deposition profile can be achieved by blending particles of different sizes with an appropriate mixing ratio. While the *in vivo* prophylactic efficiency of dual targeting WKS13 formulation has been demonstrated in the current study using hamsters as model, future work will focus on examining the pharmacokinetic profile of the dual targeting formulations and their therapeutic efficacy against different variants of SARS-CoV-2 as well as other respiratory viruses. Moreover, further investigation on mixing mechanism will be conducted to optimise the mixing parameters for long-term formulation stability.

CRediT authorship contribution statement

Han Cong Seow: Conceptualization, Methodology, Formal analysis, Investigation, Visualization, Writing – original draft. **Jian-Piao Cai:** Methodology, Formal analysis, Investigation, Writing – review & editing. **Harry Weijie Pan:** Investigation. **Cuiting Luo:** Investigation. **Kun Wen:** Resources. **Jianwen Situ:** Investigation. **Kun Wang:** Investigation. **Hehe Cao:** Investigation. **Susan W.S. Leung:** Writing – review & editing. **Shuofeng Yuan:** Conceptualization, Validation, Writing – review & editing, Supervision, Funding acquisition. **Jenny K.W. Lam:** Conceptualization, Validation, Writing – original draft, Supervision, Project administration, Funding acquisition.

Data availability

Data will be made available on request.

Acknowledgements

The study was financially supported by the Health and Medical Fund (HMRF 20190582, 19180502), HMRF Fellowship (07210107), Food and Health Bureau; National Natural Science Foundation of China (NSFC)/ Research Grants Council (RGC) Joint Research Scheme (N_HKU767/22); Hong Kong PhD Fellowship (PF18–13277), RGC, Hong Kong; and the Health@InnoHK program of the Innovation and Technology Commission of the Hong Kong SAR Government. The authors thank Mr. Ray Lee (Department of Pharmacology and Pharmacy, HKU) for his kind assistance with the TGA experiments.

Appendix A. Supplementary data

Supplementary data to this article can be found online at https://doi.org/10.1016/j.jconrel.2023.04.029.

References

[1] L.L. Chen, S.M.U. Abdullah, W.M. Chan, B.P. Chan, J.D. Ip, A.W. Chu, L. Lu, X. Zhang, Y. Zhao, V.W. Chuang, A.K. Au, V.C. Cheng, S. Sridhar, K.Y. Yuen, I. F. Hung, K.H. Chan, K.K. To, Contribution of low population immunity to the severe omicron BA.2 outbreak in Hong Kong, Nat. Commun. 13 (2022) 3618.
[2] B.M. Prubeta, Variants of SARS CoV-2: mutations, transmissibility, virulence, drug resistance, and antibody/vaccine sensitivity, Front. Biosci. (Landmark Ed.) 27 (2022) 65.
[3] D. Focosi, M. Tuccori, Prescription of anti-spike monoclonal antibodies in COVID-19 patients with resistant SARS-CoV-2 variants in Italy, Pathogens 11 (2022).
[4] M. Cascella, M. Rajnik, A. Aleem, S.C. Dulebohn, R. Di Napoli, Features, Evaluation, and Treatment of Coronavirus (COVID-19), StatPearls, Treasure Island (FL), 2022.
[5] P.C. Taylor, A.C. Adams, M.M. Hufford, I. de la Torre, K. Winthrop, R.L. Gottlieb, Neutralizing monoclonal antibodies for treatment of COVID-19, Nat. Rev. Immunol. 21 (2021) 382–393.
[6] N. Kreuzberger, C. Hirsch, K.L. Chai, E. Tomlinson, Z. Khosravi, M. Popp, M. Neidhardt, V. Piechotta, S. Salomon, S.J. Valk, I. Monsef, C. Schmaderer, E. M. Wood, C. So-Osman, D.J. Roberts, Z. McQuilten, L.J. Estcourt, N. Skoetz, SARS-CoV-2-neutralising monoclonal antibodies for treatment of COVID-19, Cochrane Database Syst. Rev. 9 (2021) (CD013825).
[7] M.Z. Tay, C.M. Poh, L. Renia, P.A. MacAry, L.F.P. Ng, The trinity of COVID-19: immunity, inflammation and intervention, Nat. Rev. Immunol. 20 (2020) 363–374.
[8] M.S. Piepenbrink, J.G. Park, F.S. Oladunni, A. Deshpande, M. Basu, S. Sarkar, A. Loos, J. Woo, P. Lovalenti, D. Sloan, C. Ye, K. Chiem, C.W. Bates, R.E. Burch, N. B. Erdmann, P.A. Goepfert, V.L. Truong, M.R. Walter, L. Martinez-Sobrido, J. J. Kobie, Therapeutic activity of an inhaled potent SARS-CoV-2 neutralizing human monoclonal antibody in hamsters, Cell Rep. Med. 2 (2021), 100218.
[9] X. Zhang, H. Zhang, T. Li, S. Chen, F. Luo, J. Zhou, P. Zheng, S. Song, Y. Wu, T. Jin, N. Tang, A. Jin, C. Yang, G. Cheng, R. Gong, S. Chiu, A. Huang, A potent neutralizing antibody provides protection against SARS-CoV-2 omicron and Delta variants via nasal delivery, Signal. Transduct. Target. Ther. 7 (2022) 301.
[10] X. Cao, J. Maruyama, H. Zhou, Y. Fu, L. Kerwin, C. Powers, R.A. Sattler, J. T. Manning, A. Singh, R. Lim, L.D. Healy, S. Johnson, E. Paz Cabral, D. Li, L. Lu, A. Ledesma, D. Lee, S. Richards, L. Rivero-Nava, Y. Li, W. Shen, K. Stegman, B. Blair, S. Urata, M. Kishimoto-Urata, J. Ko, N. Du, K. Morais, K. Lawrence, I. Rivera, C.I. Pai, D. Bresson, M. Brunswick, Y. Zhang, H. Ji, S. Paessler, R.D. Allen, Unbiased approach to identify and assess efficacy of human SARS-CoV-2 neutralizing antibodies, Sci. Rep. 12 (2022) 15517.
[11] A.N. Hegazy, J. Kronke, S. Angermair, S. Schwartz, C. Weidinger, U. Keller, S. Treskatsch, B. Siegmund, T. Schneider, Anti-SARS-CoV2 antibody-mediated cytokine release syndrome in a patient with acute promyelocytic leukemia, BMC Infect. Dis. 22 (2022) 537.
[12] H.C. Seow, Q. Liao, A.T.Y. Lau, S.W.S. Leung, S. Yuan, J.K.W. Lam, Dual targeting powder formulation of antiviral agent for customizable nasal and lung deposition profile through single intranasal administration, Int. J. Pharm. 619 (2022), 121704.
[13] H.W. Pan, H.C. Seow, J.C.K. Lo, J. Guo, L. Zhu, S.W.S. Leung, C. Zhang, J.K. W. Lam, Spray-dried and spray-freeze-dried powder formulations of an anti-interleukin-4Ralpha antibody for pulmonary delivery, Pharm. Res. 39 (2022) 2291–2304.
[14] T. Serno, R. Geidobler, G. Winter, Protein stabilization by cyclodextrins in the liquid and dried state, Adv. Drug Deliv. Rev. 63 (2011) 1086–1106.
[15] M.Y.T. Chow, Y. Qiu, F.F.K. Lo, H.H.S. Lin, H.K. Chan, P.C.L. Kwok, J.K.W. Lam, Inhaled powder formulation of naked siRNA using spray drying technology with l-leucine as dispersion enhancer, Int. J. Pharm. 530 (2017) 40–52.
[16] J.C.K. Lo, H.W. Pan, J.K.W. Lam, Inhalable protein powder prepared by spray-freeze-drying using Hydroxypropyl-beta-Cyclodextrin as excipient, Pharmaceutics 13 (2021) 615.
[17] C.P. Ong, Z.W. Ye, K. Tang, R. Liang, Y. Xie, H. Zhang, Z. Qin, H. Sun, T.Y. Wang, Y. Cheng, H. Chu, J.F. Chan, D.Y. Jin, S. Yuan, Comparative analysis of SARS-CoV-2 omicron BA.2.12.1 and BA.5.2 variants, J. Med. Virol. 95 (2022), e28326.
[18] Y. Qiu, Q. Liao, M.Y.T. Chow, J.K.W. Lam, Intratracheal Administration of dry Powder Formulation in mice, J. Vis. Exp. 161 (2020), e61469.
[19] Y. Qiu, R.C.H. Man, Q. Liao, K.L.K. Kung, M.Y.T. Chow, J.K.W. Lam, Effective mRNA pulmonary delivery by dry powder formulation of PEGylated synthetic KL4 peptide, J. Control. Release 314 (2019) 102–115.
[20] R. Scherliess, M. Monckedieck, K. Young, S. Trows, S. Buske, S. Hook, First in vivo evaluation of particulate nasal dry powder vaccine formulations containing ovalbumin in mice, Int. J. Pharm. 479 (2015) 408–415.
[21] S. Yuan, R. Wang, J.F. Chan, A.J. Zhang, T. Cheng, K.K. Chik, Z.W. Ye, S. Wang, A. C. Lee, L. Jin, H. Li, D.Y. Jin, K.Y. Yuen, H. Sun, Metallodrug ranitidine bismuth citrate suppresses SARS-CoV-2 replication and relieves virus-associated pneumonia in Syrian hamsters, Nat. Microbiol. 5 (2020) 1439–1448.
[22] S. Yuan, Z.W. Ye, R. Liang, K. Tang, A.J. Zhang, G. Lu, C.P. Ong, V.K. Man Poon, C. C. Chan, B.W. Mok, Z. Qin, Y. Xie, A.W. Chu, W.M. Chan, J.D. Ip, H. Sun, J. O. Tsang, T.T. Yuen, K.K. Chik, C.C. Chan, J.P. Cai, C. Luo, L. Lu, C.C. Yip, H. Chu, K.K. To, H. Chen, D.Y. Jin, K.Y. Yuen, J.F. Chan, Pathogenicity, transmissibility, and fitness of SARS-CoV-2 omicron in Syrian hamsters, Science 377 (2022) 428–433.
[23] S. Yuan, B. Yan, J. Cao, Z.W. Ye, R. Liang, K. Tang, C. Luo, J. Cai, H. Chu, T. W. Chung, K.K. To, I.F. Hung, D.Y. Jin, J.F. Chan, K.Y. Yuen, SARS-CoV-2 exploits host DGAT and ADRP for efficient replication, Cell Discov. 7 (2021) 100.
[24] A.J. Zhang, A.C. Lee, H. Chu, J.F. Chan, Z. Fan, C. Li, F. Liu, Y. Chen, S. Yuan, V. K. Poon, C.C. Chan, J.P. Cai, K.L. Wu, S. Sridhar, Y.S. Chan, K.Y. Yuen, Severe acute respiratory syndrome coronavirus 2 infects and damages the mature and immature olfactory sensory neurons of hamsters, Clin. Infect. Dis. 73 (2021) e503–e512.
[25] A.C. Lee, A.J. Zhang, J.F. Chan, C. Li, Z. Fan, F. Liu, Y. Chen, R. Liang, S. Sridhar, J. P. Cai, V.K. Poon, C.C. Chan, K.K. To, S. Yuan, J. Zhou, H. Chu, K.Y. Yuen, Oral SARS-CoV-2 inoculation establishes subclinical respiratory infection with virus shedding in Golden Syrian hamsters, Cell Rep. Med. 1 (2020), 100121.
[26] S. Yuan, H. Chu, J. Huang, X. Zhao, Z.W. Ye, P.M. Lai, L. Wen, J.P. Cai, Y. Mo, J. Cao, R. Liang, V.K. Poon, K.H. Sze, J. Zhou, K.K. To, Z. Chen, H. Chen, D.Y. Jin, J. F. Chan, K.Y. Yuen, Viruses harness YxxO motif to interact with host AP2M1 for replication: A vulnerable broad-spectrum antiviral target, Sci. Adv. 6 (2020) eaba7910.
[27] H.A. Parray, S. Shukla, R. Perween, R. Khatri, T. Shrivastava, V. Singh, P. Murugavelu, S. Ahmed, S. Samal, C. Sharma, S. Sinha, K. Luthra, R. Kumar, Inhalation monoclonal antibody therapy: a new way to treat and manage respiratory infections, Appl. Microbiol. Biotechnol. 105 (2021) 6315–6332.
[28] M.K. Wynia, L.E. Beaty, T.D. Bennett, N.E. Carlson, C.B. Davis, B.M. Kwan, D. A. Mayer, T.C. Ong, S. Russell, J.D. Steele, H.R. Stocker, A.F. Wogu, R.D. Zane, R. J. Sokol, A.A. Ginde, Real-world evidence of neutralizing monoclonal antibodies for preventing hospitalization and mortality in COVID-19 outpatients, Chest (2022). In press.
[29] M.Y.T. Chow, H.W. Pan, H.C. Seow, J.K.W. Lam, Inhalable neutralizing antibodies - promising approach to combating respiratory viral infections, Trends Pharmacol. Sci. 44 (2023) 85–97.
[30] Q. Wang, Y. Guo, S. Iketani, M.S. Nair, Z. Li, H. Mohri, M. Wang, J. Yu, A. D. Bowen, J.Y. Chang, J.G. Shah, N. Nguyen, Z. Chen, K. Meyers, M.T. Yin, M. E. Sobieszczyk, Z. Sheng, Y. Huang, L. Liu, D.D. Ho, Antibody evasion by SARS-

CoV-2 omicron subvariants BA.2.12.1, BA.4 and BA.5, Nature 608 (2022) 603–608.
[31] C. Cruz-Teran, K. Tiruthani, M. McSweeney, A. Ma, R. Pickles, S.K. Lai, Challenges and opportunities for antiviral monoclonal antibodies as COVID-19 therapy, Adv. Drug Deliv. Rev. 169 (2021) 100–117.
[32] K.B. Shepard, D.T. Vodak, P.J. Kuehl, D. Revelli, Y. Zhou, A.M. Pluntze, M.S. Adam, J.C. Oddo, L. Switala, J.L. Cape, J.M. Baumann, M. Banks, Local treatment of non-small cell lung Cancer with a spray-dried bevacizumab formulation, AAPS PharmSciTech 22 (2021) 230.
[33] H. Wang, P. Connaughton, K. Lachacz, N. Carrigy, M. Ordoubadi, D. Lechuga-Ballesteros, R. Vehring, Inhalable microparticle platform based on a novel shell-forming lipid excipient and its feasibility for respirable delivery of biologics, Eur. J. Pharm. Biopharm. 177 (2022) 308–322.
[34] E. Hartl, G. Winter, A. Besheer, Influence of hydroxypropyl-Beta-cyclodextrin on the stability of dilute and highly concentrated immunoglobulin g formulations, J. Pharm. Sci. 102 (2013) 4121–4131.
[35] M. Gomez, J. McCollum, H. Wang, M. Ordoubadi, C. Jar, N.B. Carrigy, D. Barona, I. Tetreau, M. Archer, A. Gerhardt, C. Press, C.B. Fox, R.M. Kramer, R. Vehring, Development of a formulation platform for a spray-dried, inhalable tuberculosis vaccine candidate, Int. J. Pharm. 593 (2021), 120121.
[36] N. Alhajj, N.J. O'Reilly, H. Cathcart, Leucine as an excipient in spray dried powder for inhalation, Drug Discov. Today 26 (2021) 2384–2396.
[37] M. Degenhard, W. Gerallt, B. Matthias, Intranasal drug administration — An attractive delivery route for some drugs, in: V. Omboon, O. Suleiman (Eds.), Drug Discovery and Development, IntechOpen, Rijeka, 2015. Ch. 13.
[38] S. Focaroli, P.T. Mah, J.E. Hastedt, I. Gitlin, S. Oscarson, J.V. Fahy, A.M. Healy, A Design of Experiment (DoE) approach to optimise spray drying process conditions for the production of trehalose/leucine formulations with application in pulmonary delivery, Int. J. Pharm. 562 (2019) 228–240.
[39] W. Sungnak, N. Huang, C. Bécavin, M. Berg, R. Queen, M. Litvinukova, C. Talavera-López, H. Maatz, D. Reichart, F. Sampaziotis, K.B. Worlock, M. Yoshida, J. L. Barnes, N.E. Banovich, P. Barbry, A. Brazma, J. Collin, T.J. Desai, T.E. Duong, O. Eickelberg, C. Falk, M. Farzan, I. Glass, R.K. Gupta, M. Haniffa, P. Horvath, N. Hubner, D. Hung, N. Kaminski, M. Krasnow, J.A. Kropski, M. Kuhnemund, M. Lako, H. Lee, S. Leroy, S. Linnarson, J. Lundeberg, K.B. Meyer, Z. Miao, A. V. Misharin, M.C. Nawijn, M.Z. Nikolic, M. Noseda, J. Ordovas-Montanes, G. Y. Oudit, D. Pe'er, J. Powell, S. Quake, J. Rajagopal, P.R. Tata, E.L. Rawlins, A. Regev, P.A. Reyfman, O. Rozenblatt-Rosen, K. Saeb-Parsy, C. Samakovlis, H. B. Schiller, J.L. Schultze, M.A. Seibold, C.E. Seidman, J.G. Seidman, A.K. Shalek, D. Shepherd, J. Spence, A. Spira, X. Sun, S.A. Teichmann, F.J. Theis, A.M. Tsankov, L. Vallier, M. van den Berge, J. Whitsett, R. Xavier, Y. Xu, L.-E. Zaragosi, D. Zerti, H. Zhang, K. Zhang, M. Rojas, F. Figueiredo, H.C.A.L.B, Network, SARS-CoV-2 entry factors are highly expressed in nasal epithelial cells together with innate immune genes, Nat. Med. 26 (2020) 681–687.
[40] Y.J. Hou, K. Okuda, C.E. Edwards, D.R. Martinez, T. Asakura, K.H. Dinnon III, T. Kato, R.E. Lee, B.L. Yount, T.M. Mascenik, G. Chen, K.N. Olivier, A. Ghio, L. V. Tse, S.R. Leist, L.E. Gralinski, A. Schäfer, H. Dang, R. Gilmore, S. Nakano, L. Sun, M.L. Fulcher, A. Livraghi-Butrico, N.I. Nicely, M. Cameron, C. Cameron, D. J. Kelvin, A. de Silva, D.M. Margolis, A. Markmann, L. Bartelt, R. Zumwalt, F. J. Martinez, S.P. Salvatore, A. Borczuk, P.R. Tata, V. Sontake, A. Kimple, I. Jaspers, W.K. O'Neal, S.H. Randell, R.C. Boucher, R.S. Baric, SARS-CoV-2 reverse genetics reveals a variable infection gradient in the respiratory tract, Cell 182 (2020) 429–446.e414.
[41] T.D. Rogers, B. Button, S.N.P. Kelada, L.E. Ostrowski, A. Livraghi-Butrico, M. I. Gutay, C.R. Esther, B.R. Grubb, Regional differences in Mucociliary clearance in the upper and lower airways, Front. Physiol. 13 (2022).
[42] A. Baldelli, M.A. Boraey, H. Oguzlu, A. Cidem, A.P. Rodriguez, H.X. Ong, F. Jiang, M. Bacca, A. Thamboo, D. Traini, A. Pratap-Singh, Engineered nasal dry powder for the encapsulation of bioactive compounds, Drug Discov. Today 27 (2022) 2300–2308.